Unknown input observer design for lithium-ion batteries SOC estimation based on a differential-algebraic model

Jamila Snoussi, Seifeddine Ben Elghali, Mohamed Zerrougui, Michel Bensoam, Mohamed Benbouzid, Mohamed Mimouni

Unknown Input Observer Design for Lithium-ion Batteries SOC Estimation based on a Differential-Algebraic Model

Jamila Snoussi[a], Seifeddine Ben Elghali[b], Mohamed Zerrougui[b], Michel Bensoam[b], Mohamed Benbouzid[c,*], Mohamed Faouzi Mimouni[a]

[a] *Engineering School of Monastir (ENIM), Monastir University, Monastir, Tunisia*
[b] *Laboratory of Information and Systems (LIS-UMR CNRS 7020), Aix-Marseille University, Marseille, France*
[c] *University of Brest, UMR CNRS 6027 IRDL, Brest, France and with the Shanghai Maritime University, 201306, Shanghai, China*

Abstract

An accurate battery management strategy is a crucial need in the developing of reliable and viable plug in and hybrid electric vehicles. This on-board algorithm has the advantages to protect the battery from critical operating conditions and improve its lifetime. However, the effectiveness of the battery management strategy mainly depends on the accuracy of its state of charge (SOC). In this context, this paper proposes a novel technique for the SOC estimation based on the unknown input observer and a new differential-algebraic model of a lithium iron phosphate battery. The proposed observer aims to overcome the unknown value of the initial SOC for on-board batteries using only current and terminal voltage measurements. A reduced-order based unknown input observer is developed to estimate the open circuit voltage and the SOC using the OCV-SOC characteristic offline-determined. The unbiasedness of the estimation error is guaranteed by the parameterization of a set of Sylvester constraints. The performance of the proposed observer is verified by simulations and experiments and the accuracy of the obtained results is analyzed and assessed.

*Corresponding author

Email addresses: snoussijamila@yahoo.fr (Jamila Snoussi), seifeddine.benelghali@lis-lab.fr (Seifeddine Ben Elghali), mohamed.zerrougui@lis-lab.fr (Mohamed Zerrougui), mohamed.benbouzid@univ-brest.fr (Mohamed Benbouzid), mfaouzi.mimouni@enim.rnu.tn (Mohamed Faouzi Mimouni)

Keywords: Differential-algebraic systems, Lithium-ion battery, State of charge, SOC estimation, Unknown input observer.

1. Introduction

Electrochemical batteries have presented an attractive alternative energy source in automotive applications for several years [1]. Electric and Hybrid Electric Vehicles (EV/HEV) have proven ability towards reducing harmful gas emissions and securing natural resources [2], and as a result, battery technologies have experienced significant global growth, which has led to the production of lithium-ion cells with high power and energy densities, long life cycles, wide ranges of operating temperature, and low self-discharge rate [3],[4]. These benefits have led to Lithium-Ion Batteries (LIB) being preferable to lead acid and nickel metal batteries. To date, LIB is among the most popular Energy Storage Systems (ESS) used in powertrain applications [5].

The cost efficiency and the lifetime (durability) of LIB mainly depend on the battery management strategy. This management algorithm is used to secure the device from unsafe operation (over charge, over discharge, high charge and discharge current rate) [6] as well as to optimize the battery reliability [7]. An important prerequisite of this algorithm is to have an accurate estimation of the battery State of Charge (SOC). This energy indicator provides information on the available capacity in the storage device and has the same role as fuel gauges in conventional internal combustion engine.

In fact, online estimation of batteries SOC is a challenging issue in electric and hybrid vehicles. This is mainly due to high dynamic operation as well as nonlinearities in the batteries behavior. Several approaches and algorithms of SOC estimation have been reported in [8], [9], [10]. Among estimation techniques, the most conventional is the Coulomb counting also called Ampere-hour (Ah) counting method [11]. This approach is based on the integration of the battery current over time under charge and discharge modes. It requires a very low computing power and can predict battery SOC in real time operation. But, to be efficiently used this open loop technique requires a known initial SOC. Furthermore, accumulated measurement errors and noise can significantly affect the accuracy of the algorithm. Another approach is based on the open circuit voltage (OCV) measurement [12], [13]. The relationship between the battery OCV and SOC, often loaded in a look up table, allows for the estimation of battery SOC with a simple measurement of the voltage under open circuit conditions. The OCV-SOC characteristic has the advantage to present slight changes over battery lifetime[12], [14]. However, a long relaxation time (rest period) is needed to reach equilibrium state (a range of hours) [15], which enables it to predict on-board batteries SOC. This method can also be used in combination with the Ah counting method [16] but it is still an off-line estimation technique.

The impedance spectroscopy-based estimation [17], [18] is also not suitable for online applications due to the influence of temperature and cell aging on the LIB impedance [19]. Usually, the sensitivity of the internal impedance parameters on temperature is extremely higher than that on SOC [20].

In [21], a Fuzzy Logic (FL) techniques is proposed to estimate the battery SOC. In fact, all the proposed FL-based methods are used in combination with other estimation techniques [21], [22]. They involve a relationship between the SOC and another indicator parameters such as the electric impedance characteristic taking, consequently, the same underlying constraints of the respective methodology. The Neural Network (NN) technique proposed in [23], [24] presents an interesting alternative for SOC estimation. This algorithm is based on a NN model of the battery, which is used to predict the SOC without knowledge of the system behavior. But, developing a NN algorithm requires a large amount of data and is limited for operating conditions covered by the training data [25].

Recently, SOC estimation methodologies based on battery models have increasingly been related to EV real time operation due to their reliability and ability to describe complex behavior of LIBs [26], [27]. Model-based estimation techniques can be applied directly or together with adaptive filters and observers [28], where the common idea is to deploy an accurate model of the battery (electric, electrochimical or mathematical) and measured signals (voltage, current, temperature) to estimate the SOC. In direct methods [13], the battery is modeled in a simple electric circuit and a mathematical model is used to calculate the SOC. But, the efficiency of direct methods relies solely on the accuracy of the mathematical model.

In order to perform real time SOC estimation using model-based approaches, filter based-algorithms such as Kalman Filter (KF) and its variants are involved in the estimation process [10],[29],[30],[31]. In fact, the ordinary KF is not suitable for nonlinear state estimations. Its first derivative, the Extended Kalman Filter (EKF) is applied in a variety of applications with different battery models [10], [24] but it presents the same drawback of the KF as it linearizes models nonlinearities. The modern Sigma-Point Kalman Filter (SPKF) has been developed to surmount disadvantages of model linearization. Its performances are reliant to the initial SOC value, which is seldom available on-board [32]. Unscented Kalman Filters (UKF) need important computing power compared to other Kalman filters [33].

Other proposed methodologies are also reported and discussed in [34], such as hybrid techniques combining two or three algorithms to estimate the SOC. These techniques take the advantage of each method to obtain optimal performance. Moreover, it can been concluded from the comparison study provided in [34] that some simpler methods such as KF and EKF can be more accurate than hybrid approaches and require smaller memory device.

In reference [35], the authors provided an Adaptive Particle Filter (APF) to estimate the SOC and proved its superiority compared to the conventional PF [36],[34]. Other advanced techniques of adaptive observers are also provided in [37] using a new adaptive fading EKF and in [38] using an adaptive Sliding Mode Observer (SMO). For the adaptive SMO, it was difficult to adjust switching gains to control sliding regime and it was noticed that the convergence time highly depends on the initial SOC.

Another issue for SOC estimation is the battery model choice and parameter identification. In fact, majority of the existing researches used offline identification methods to calculate a fixed set of parameters that will be used in the estimation process [39], [40]. However, many factors such as temperature, aging, and operation conditions could significantly impact the LIB characteristics and then the model parameters as well as the SOC estimation [41].

Depending on the targeted accuracy, a variety of models have been developed for LIBs. In EVs, electric circuit-based models are the most suitable to describe dynamic behavior of a battery in charge and discharge modes [42], [43]. Some researchers used a simple Rint model consisting of a constant voltage source OCV in series with a resistance [44]. To consider the relaxation phenomena during or after charging/discharging cycles, a parallel RC element needs to be added in the circuit (Thevenin model) [45], [46]. For more accurate results, more than one RC branch are recommended [47]. However, it should be mentioned that during rest periods the real battery OCV should not be constant and is still changing to reach an equilibrium level. Constant voltage source-based models are unfortunately unable to track these changes when a current is not circulating through the battery.

In this context, this paper proposes a new battery model and a novel approach to estimate the battery SOC using the Unknown Input Observer (UIO) and the OCV-SOC characteristic curve. With respect to the above-discussed works, the salient features of the paper proposal can be summarized as follows:

1. Proposing a modified Thevenin circuit for Lithium batteries to consider OCV variations during operation and resting periods.

2. Online model parameters determination and updating to track changes caused by temperature variations, vehicle operation mode, and battery aging..

3. Developing a new SOC estimation approach based on an unknown input observer and a new differential-algebraic model to overcome problems of unknown initial SOC, OCV measurements, and computational burden.

4. Estimating the SOC using only measurements issued from hardware normally connected to the battery in real-world applications.

The proposed new battery model and its SOC estimation technique are both validated by simulations and experiments using two different load profiles. Finally, it is worthy to mention that the proposal could be used for any battery technology.

This paper is organized as follows: in Section II, an equivalent circuit-based model and an online identification parameter is introduced. In Section III, the observer statement used for the SOC estimation is described. In Section IV, the verification in terms of model accuracy and the experimental validation of the proposed estimation method are presented. Finally, the paper is concluded in Section V.

2. Battery model identification

2.1. Equivalent circuit model

Reducing computational efforts in online estimation tasks is important. The comparative study developed in [48] shows the performance (robustness, accuracy, and simplicity) of the first order RC-model compared to other complex models for two types of battery cells.
The equivalent circuit model selected for this application is given in Fig. 1. Contrarily to typical Thevenin model, a capacity C_0 is used instead of constant voltage source to reproduce the battery charge and discharge behaviors [49]. The internal resistance R_0 is resulting from the electrolyte in which the battery electrodes are immersed while the parallel R_1C_1 highlights the rest time effect on the battery response. The related parameters are determined in section 4. This adopted model should be enough effective for real time estimation.

2.2. Online parameter identification

To identify the model parameters, a recursive least square (RLS) method is adopted. Simplicity and fast convergence are the main advantages of this algorithm compared to other identification techniques. It offers the ability to

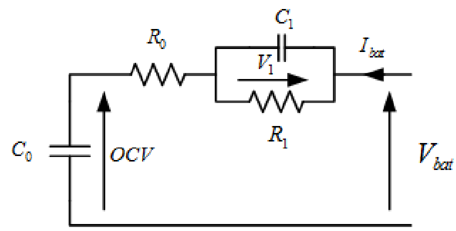

Figure 1: Battery model

perform online identification tasks [50]. By using Kirchhoff's laws, the equivalent circuit given by Fig.1 leads to the following equations:

$$V_{bat} = OCV + V_1 + V_{R_0} \tag{1}$$

$$\frac{dSOC}{dt} = \frac{1}{C_n} I_{bat} \tag{2}$$

$$\frac{dV_1}{dt} = -\frac{1}{R_1 C_1} V_1 + \frac{1}{C_1} I_{bat} \tag{3}$$

where C_n is the nominal capacity, in Ah, of the battery. To identify R_1, C_0, R_1 and C_1 we formulate the transfer function $H(s)$ between the terminal battery voltage V_{bat} and the current I_{bat}, then we obtain

$$H(s) = \frac{V_{bat}}{I_{bat}} = \frac{R_1}{R_1 C_1 s + 1} + \frac{1}{C_0 s} + R_0 \tag{4}$$

then, the transfer function has the following general form

$$H(s) = \frac{a_2 s^2 + a_1 s + a_0}{s^2 + b_0 s} \tag{5}$$

where

$$\begin{cases} a_2 = R_0; a_1 = \frac{R_0}{R_1 C_1} + \frac{1}{C_0} + \frac{1}{C_1}; a_0 = \frac{1}{R_1 C_1 C_0} \\ b_0 = \frac{1}{R_1 C_1} \end{cases} \tag{6}$$

Using the following bilinear transformation [51]

$$s \to \frac{2}{T_S} \left(\frac{1 - z^{-1}}{1 + z^{-1}} \right) \tag{7}$$

with T_s is the sampling time, the discretization of $H(s)$ is given by

$$H(z) = \frac{V_{bat}(z)}{I_{bat}(z)} = \frac{c_0 + c_1 z^{-1} + c_2 z^{-2}}{1 + d_1 z^{-1} + d_2 z^{-2}} \tag{8}$$

where

$$\begin{cases} c_0 = \frac{2a_1T_s+a_0T_s^2+4a_2}{2b_0T_s+4} \\ c_1 = \frac{-a_2+a_0T_s^2}{b_0T_s+2} \\ c_2 = \frac{4a_2-2a_1T_s+a_0T_s^2}{2b_0T_s} \\ d_1 = \frac{-4}{b_0T_s+2} \\ d_2 = \frac{2-b_0T_s}{2+b_0T_s} \end{cases} \tag{9}$$

Based on these parameters, we can develop the recurrent equation of the system as follows

$$\begin{aligned} &V_{bat}(k) = -d_1V_{bat}(k-1) - d_2V_{bat}(k-2) + c_0I_{bat}(k) + \\ &c_1I_{bat}(k-1) + c_2I_{bat}(k-2) \end{aligned} \tag{10}$$

which can be written as

$$V_{bat}(k) = \Phi^T(k)\theta(k-1) \tag{11}$$

where V_{bat} is the measured voltage vector

$$\Phi = \begin{bmatrix} -V_{bat}(k-1) \\ -V_{bat}(k-2) \\ I_{bat}(k) \\ I_{bat}(k-1) \\ I_{bat}(k-2) \end{bmatrix} \tag{12}$$

is the regressors vector, and

$$\theta = \begin{bmatrix} d_1 & d_2 & c_0 & c_1 & c_2 \end{bmatrix}^T \tag{13}$$

is the vector of the unknown coefficients to be determined.

Disposing of a set of n measurements of the battery voltage, the objective of the RLS is to iteratively minimize, the following quadratic error

$$e = \frac{1}{n}\sum_{k=1}^{n}\left[V_{bat}(k) - \Phi^T(k)\theta(k-1)\right]^2 \tag{14}$$

in order to estimate the vector
$\hat{\theta} = \begin{bmatrix} \hat{d}_1 & \hat{d}_2 & \hat{c}_0 & \hat{c}_1 & \hat{c}_2 \end{bmatrix}^T$.
From $\hat{\theta}$, we can calculate ($\hat{\mathrm{R}}_0$,$\hat{\mathrm{C}}_0$,$\hat{\mathrm{R}}_1$and$\hat{\mathrm{C}}_1$).

3. SOC Estimation

SOC estimation algorithms typically require intensive computational efforts due to many involved parameters and partial differential equations. Appropriate simplifications are therefore necessary to facilitate a real time implementation. In the current implementation a reduced-order UIO approach is used in order to minimize the computational time and simplify the algorithm matrices computing. Some interesting theoretical results on UIO are presented in [52] for a linear case, in [53] for a bilinear system and in [54] and [55] for a nonlinear case.

The battery model is written as a differential-algebraic systems, including by adding the OCV-SOC nonlinear characteristic equation. It can be noticed that the relationship between the OCV and SOC can be approximated by a linear interpolation in the interval between 10% and 90% (Fig.(5)) and can be written as $OCV = a.SOC + b$.

With this algebraic equation, we obtain the following linear descriptor system

$$\bar{\mathbf{E}}\dot{\bar{x}} = \bar{\mathbf{A}}\bar{x} + \bar{b} + \bar{\mathbf{B}}u \tag{15a}$$

$$\bar{y} = \bar{\mathbf{C}}\bar{x} + Du \tag{15b}$$

with,

$$\bar{x} = \begin{bmatrix} V_1 \\ SOC \\ OCV \end{bmatrix},\ u = I_{bat},\ \bar{y} = V_{bat}$$

and $\bar{\mathbf{E}} = \begin{bmatrix} 1 & 0 & 0 \\ 0 & 1 & 0 \\ 0 & 0 & 0 \end{bmatrix}$, $\bar{\mathbf{A}} = \begin{bmatrix} \frac{-1}{R_1 C_1} & 0 & 0 \\ 0 & 0 & 0 \\ 0 & a & -1 \end{bmatrix}$, $\bar{b} = \begin{bmatrix} 0 \\ 0 \\ b \end{bmatrix}$, $\bar{\mathbf{B}} = \begin{bmatrix} \frac{1}{C_1} \\ \frac{1}{C_n} \\ 0 \end{bmatrix}$, $\bar{\mathbf{C}} = \begin{bmatrix} 1 & 0 & 1 \end{bmatrix}$, $D = R_0$

Let us introduce the following new system including the augmented state

$x = \begin{bmatrix} \bar{x}^T & v^T \end{bmatrix}^T$ with $v = Du$, then we obtain

$$E\dot{x} = Ax + \bar{\mathbf{b}} + Bu \tag{16a}$$

$$y = Cx \tag{16b}$$

with $E = \begin{bmatrix} \bar{\mathbf{E}} & 0 \\ 0 & 0 \end{bmatrix}, A = \begin{bmatrix} \bar{\mathbf{A}} & 0 \\ 0 & -\alpha \end{bmatrix}, C = \begin{bmatrix} \bar{\mathbf{C}} & D \\ 0 & 1 \end{bmatrix}, \bar{\mathbf{b}} = \begin{bmatrix} \bar{b} \\ 0 \end{bmatrix}, B = \begin{bmatrix} \bar{\mathbf{B}} \\ \alpha D \end{bmatrix}$,

It is easy to show that, the system (16) is regular and observable i.e

$$det(sE - A) \neq 0 \quad \text{and} \quad rank \begin{bmatrix} \lambda E - A \\ C \end{bmatrix} = n \tag{17}$$

where $n = 4$ is the system's order and $(| s |, | \lambda |) \geq 1$,(s, λ) are finite.

Let us consider the following observer

$$\dot{\zeta} = \Pi_\zeta \zeta + \Pi_u u + \Pi_y y + S \tag{18a}$$

$$\hat{x} = P\zeta - QE^\perp u + My \tag{18b}$$

with $\Pi_\zeta, \Pi_u, \Pi_y, S, P, Q, M$ are matrices of appropriate dimensions to be determined, $E^\perp$ denotes a maximal row rank matrix such $E^\perp E = 0$.

Let T be a matrix of appropriate dimension such that $\varepsilon = \zeta - TEx$ be the observation error, then

its derivative is given by

$$\begin{aligned} \dot{\varepsilon} &= \dot{\zeta} - TE\dot{x} \\ &= \Pi_\zeta \varepsilon + (\Pi_\zeta TE - TA + \Pi_y C)x \\ &\quad + (\Pi_u - TB)u + (S - T\bar{\mathbf{b}}) \end{aligned} \tag{19a}$$

$$\hat{x} = P\varepsilon + (PTE + QE^\perp A + MC)x \tag{19b}$$

The problem of reduced-order observer design for the system (16) is reduced to find matrices $\Pi_\zeta, \Pi_u, \Pi_y, S, P, Q$, and M such that, the error dynamic (19) is asymptotically stable and $e = \hat{x} - x$ converges toward zero. The observation error given by (19a) converges towards zero if we choose Π_ζ $Hurwitz$ and the following generalized Sylvester matrix equations subject to T, Π_y, P, Q and M

$$\Pi_\zeta TE - TA + \Pi_y C = 0 \tag{20}$$

$$PTE + QE^\perp A + MC = I \tag{21}$$

hold, and we take

$$\Pi_u = TB \tag{22}$$

$$S = T\bar{\mathbf{b}} \tag{23}$$

If equations (20), (22), (23), (21) are satisfied, then equations (19a), (19b) become

$$\dot{\varepsilon} = \Pi_\zeta \varepsilon \tag{24}$$

$$e = P\varepsilon \tag{25}$$

if Π_ζ is Hurwitz then (24) is asymptotically stable and the error e converges toward zero. Therefore, one can choose the state observer matrix Π_ζ by using the classical theory of pole placement, with respect to the stability and the minimum settling time. In the following, we will give the solutions of equations (20) and (21), in order to compute the remaining observer matrices; Π_y, Π_u, S, P, Q and M.

The order of the observer q can be chosen between n (full order) and $n-p$ (minimum reduced-order) with $rankC = p$. The choice of the order is more easy than existing observers. In fact the choice of the order of the observer (18) directly depends on the choice of Π_ζ.

Let $N(s) \in R^{n\times r}[s]$ and $D(s) \in R^{r\times r}[s]$ be two Π_ζ^T-coprime polynomial matrices i.e $rank \begin{bmatrix} N(\lambda) \\ D(\lambda) \end{bmatrix} = r$ for any $\lambda \in \sigma(\Pi_\zeta^T)$, such that

$$(A - sE)^{-T} C^T = N(s) D^{-1}(s) \tag{26}$$

then we can write

$$N(s) = \sum_{i=0}^{w} N_i s^i \quad \text{and} \quad D(s) = \sum_{i=0}^{w} D_i s^i \tag{27}$$

with $w = max(deg\{N(s)\}, deg\{D(s)\})$

Let F and B a given matrices, for a regular pencil (E, A), the solution of the following generalized Sylvester matrix equation

$$AV - EVF = BW \tag{28}$$

with respect to V and W is given by

$$V = N_0 Z + N_1 ZF + \cdots + N_w ZF^w \tag{29}$$

$$W = D_0 Z + D_1 ZF + \cdots + D_w ZF^w \tag{30}$$

the proof of this lemma can be seen in [56].

Under (17), let Z_1 and Z_2 be two arbitrary matrices and Π_ζ a stable square matrix, the general solutions for T, Π_y, P, Q and M in equations (20) and (21) can be expressed as follows

$$T = -Z_1 N_0^T - \Pi_\zeta^T Z_1 N_1^T - \cdots - (\Pi_\zeta^w)^T Z_1 N_w^T \tag{31}$$

$$\Pi_y = -Z_1 D_0^T - \Pi_\zeta^T Z_1 D_1^T - \cdots - (\Pi_\zeta^w)^T Z_1 D_w^T \tag{32}$$

$$\begin{bmatrix} P & Q & M \end{bmatrix} = I \begin{bmatrix} TE \\ E^\perp A \\ C \end{bmatrix}^+ + Z_2 \left(I - \begin{bmatrix} TE \\ E^\perp A \\ C \end{bmatrix} \begin{bmatrix} TE \\ E^\perp A \\ C \end{bmatrix}^+ \right) \tag{33}$$

with + denotes the pseudo-inverse matrix.

Equation (20) can be written as (28). In fact, the transpose of (20) gives

$$E^T T^T \Pi_\zeta^T - A^T T^T + C^T \Pi_y^T = 0 \tag{34}$$

this equation is equivalent to (28) with $V = -T^T$ and $W = -\Pi_y^T$.

Equation (21) has the well known form $\mathcal{X}\mathcal{A} = \mathcal{B}$.
avec $\mathcal{X} = \begin{bmatrix} P & Q & M \end{bmatrix}$, $\mathcal{A} = \begin{bmatrix} (TE)^T & (E^\perp A)^T & C^T \end{bmatrix}^T$ and $\mathcal{B} = I$, the general solution in this case is given by

$$X = A^+ + Z_2(I - AA^+)$$

This completes the theorem proof.

By substituting T in (22) and (23) we obtain Π_u and S. This completes the design of the observer (18).

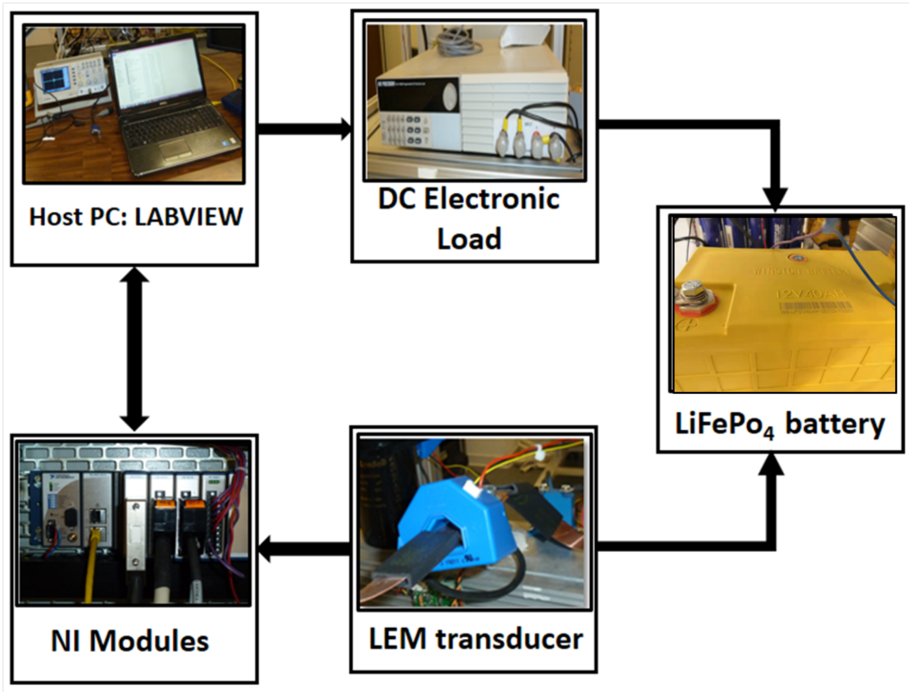

Figure 2: Test bench

4. Experimental Validation

4.1. Test bench

Experimental tests were conducted using a Lithium-iron phosphate battery ($LiFePO_4$) and a National Instruments CompactRIO platform.

The test bench (Fig. 2) consists of an LP-12V/40Ah battery from GWL Power with 12V as nominal voltage and 40Ah as nominal capacity, a battery charger SM82, a BK 8514 DC electronic load ($1200W/0-120V/0-240A$) characterized by its high accuracy and used to generate the variable load profile, a NI 9215 analog module from National Instruments (NI) having 4 channels and $16bit/100kH/\pm 10V$ of range and resolution, used for data acquisition in association with a high accurate LEM LA-205 S current transducer ($\pm 0.8\%$).

4.2. Battery model validation

The battery equivalent circuit is identified using a pulse discharge current Fig.9a and a set of battery voltage measurements Fig.9b. The RLS identification code is developed under MATLAB software then the same load profile is applied to simulate the model under MATLAB/SimPowerSystems environment. The values of the obtained parameters are given in Table 1 and the simulation results vs. measurements are presented in Fig. 4. They highlight the effectiveness of the proposed model and the identification algorithm.

Table 1: Battery model parameters (mean values)

Parameters	Values
R_0	$8.910^{-3}\Omega$
R_1	$24.110^{-3}\Omega$
C_0	$2.3110^{5}F$
C_1	$35F$

4.3. OCV-SOC curve

To construct the OCV-SOC curve, the battery is initially fully charged (100% of SOC) with a maximum voltage of $13.9V$. A pulse current load with $20A$ ($0.5C_n$) of amplitude during 10 minutes and 80 minutes of resting time is applied. The relaxation time is necessary to achieve steady-state voltage in no-load condition. The experiment is stopped when the battery cut-off voltage $V_{off} = 11V$ is reached. The total experiment duration is about 16 hours and 40 minutes where voltage and current measurements are carried out using a LABVIEW graphic interface.

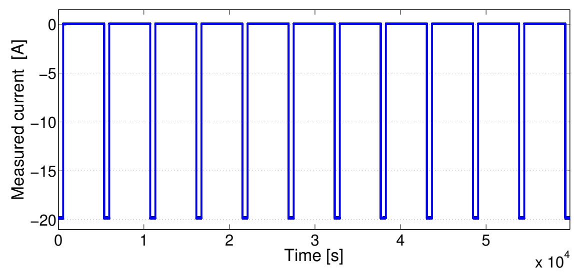

(a) Battery current

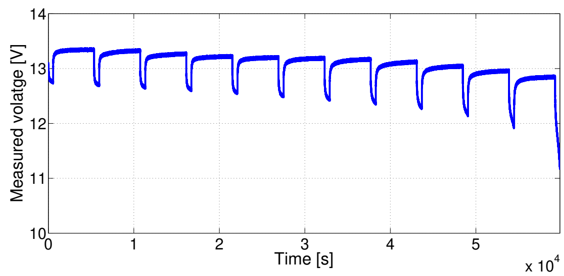

(b) Battery voltage

Figure 3: Battery discharge test: (a) Pulse discharge current (b) Measured terminal voltage

During the discharge test a set of open circuit voltage measurements are done at the end of each relaxation period. The obtained OCV-SOC curve is presented in Fig. 5.

4.4. Observer results

To validate the relevance of the proposed technique, an online SOC estimation was applied to the battery without any information on the initial SOC. The approach was verified by measurements and simulations for two load profiles and under different operating conditions. The first is the pulse discharge test and the second is the New Worldwide harmonized Light vehicles Test Procedure (WLTP), Fig. 10.

The simulation results and the experimental data for the UIO under pulse discharge test are given in figures 6 to 9. The maximum absolute error is 0.02 V for V_{bat} and much lower for V_1 and OCV. It can been noticed that the er-

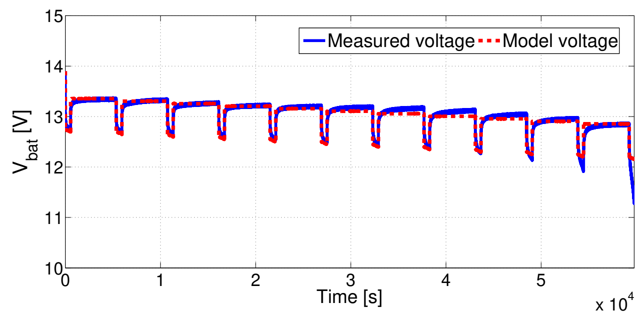

(a) Battery terminal voltage: Model voltage (dashed red) v.s measured voltage (blue)

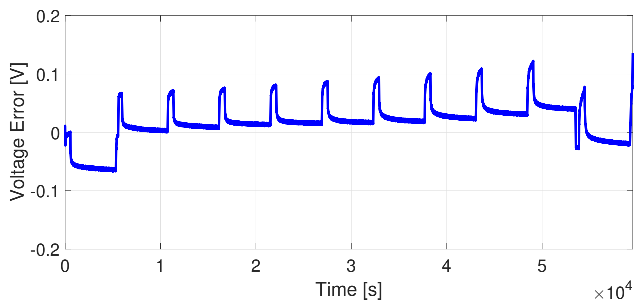

(b) Error

Figure 4: Battery model verification using pulse discharge current

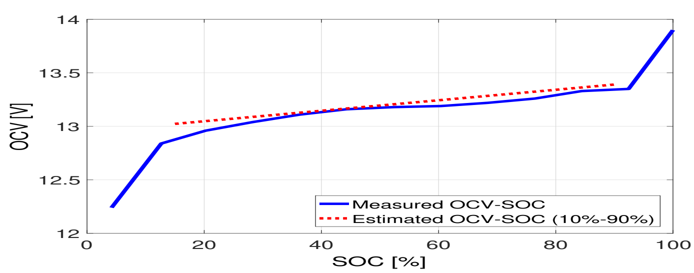

Figure 5: Measured OCV-SOC characteristic

ror computed for the SOC estimation converges to zero with lower convergence time compared to the adaptive extended Kalman filter (AEKF) and SMO [38]. Based on [37], we can notice that the UIO shows higher accuracy compared to AEKF and EKF methods. The maximum absolute SOC error given under the

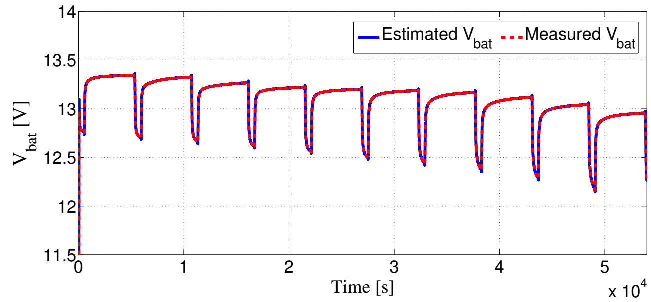

(a) Estimated and measured V_{bat}

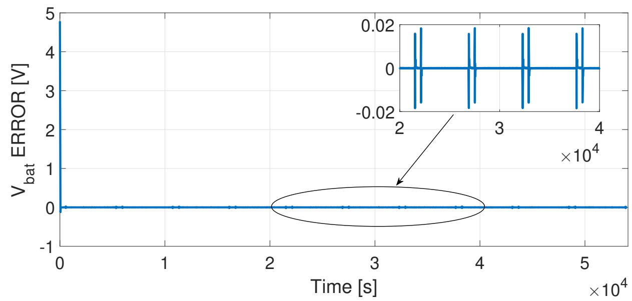

(b) Error

Figure 6: Battery terminal voltage estimation for the pulse discharge current

constant load current is 2.5% for the AEKF and 6% for the EKF.

The estimation results of the UIO under the WLTP are plotted given in Figs. 11 and 12. As it can be seen, the estimated battery SOC converges quickly, while being quite close to the measured one. The SOC estimation maximum error remains below 0.25%. This value is bigger than the pulse test maximum error due to the higher dynamic load. More estimation results are given in Table 2. Where, the initial measured SOC is 100%, $Error_{max}$ is the maximum error given for the steady state estimated SOC and $t_convergence$ is the convergence time of the proposed observer.

For comparison purposes, the proposed approach has been evaluated versus other well-known adaptive and advanced estimation techniques available in the literature, focusing on SOC estimations results under dynamic load conditions. Indeed, in[57], the authors proposed an improved adaptive SOC estimator that

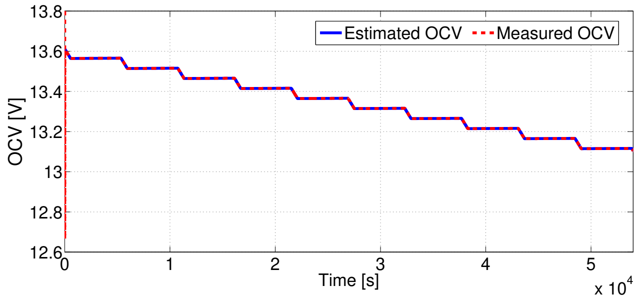

(a) Estimated and measured OCV

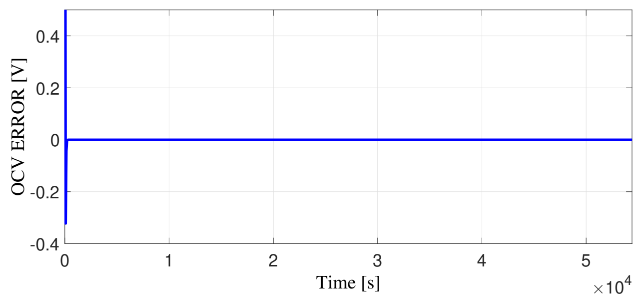

(b) Error

Figure 7: OCV estimation for the pulse discharge test

has been tested with three driving cycles, the FUDS, the DST, and the UDDS, where the lower obtained maximum error was 1.17%. In [35],the authors estimated the SOC using an adaptive PF for an UDDS driving cycle and the lower SOC error reached by this technique was 1.1%. In [38], the maximum SOC error given by the adaptive SMO was 2% and in [58], the maximum SOC error obtained by the strong tracking SPKF was 0.83%. According to the SOC estimation maximum error, it can therefore be concluded that the proposed approach is clearly outperforming the above-mentioned SOC estimation techniques.

Although the proposed technique was developed based on a simplified model, ensuring the required simplicity for real time applications, the obtained results demonstrate its relevance in accurately estimating the lithium-ion batteries SOC.

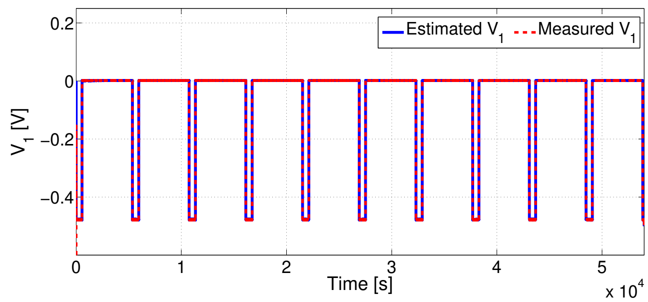

(a) Estimated and measured V_1

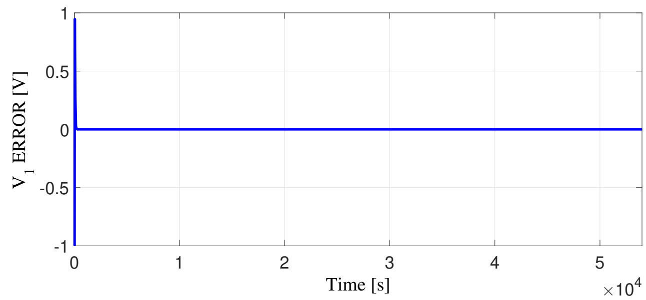

(b) Error

Figure 8: V_1 estimation for the pulse discharge test

5. Conclusion

In this paper, a first order RC model was adopted to describe the behavior of a $LiFePO_4$ battery. This model showed good performance in terms of robustness and accuracy and was enough-simple to perform real time estimation tasks. The battery measured characteristics (current and voltage) were obtained to perform model parameter identification and get the OCV-SOC curve.

Using a new differential-algebraic model for the battery, an unknown input observer based on the open circuit voltage equation was proposed to estimate the SOC. The convergence and the stability are guaranteed by using a simple pole placement. The unbiasedness of the estimation error is carried out by the parametrization of the solutions of Sylvester equations. Experimental and simulation results have clearly shown that the UIO method can estimate the battery SOC with a higher accuracy compared to Kalman filters, sliding mode

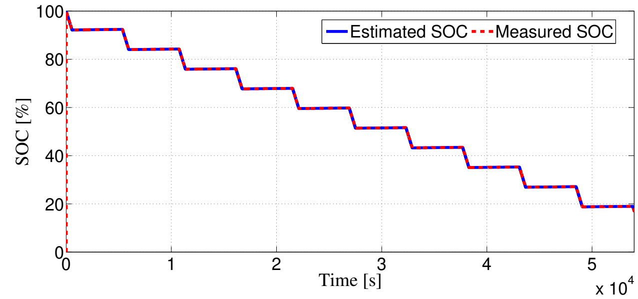

(a) Estimated and measured SOC

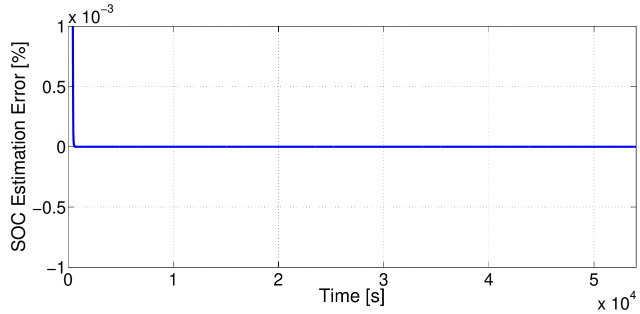

(b) Error

Figure 9: SOC estimation for the pulse discharge test

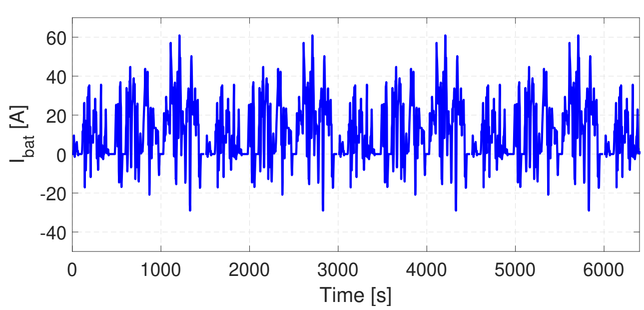

Figure 10: WLTP load current

observer, and other adaptive technique such as adaptive particle filters.
In this context, the UIO algorithm will obviously increase the effectiveness and reliability of the battery management strategy.

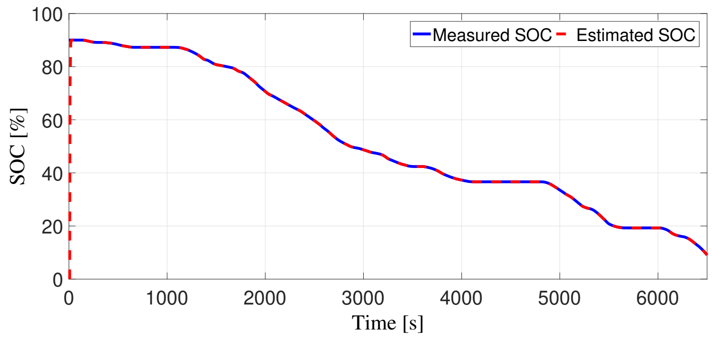

Figure 11: SOC estimation and measurement for the WLTP

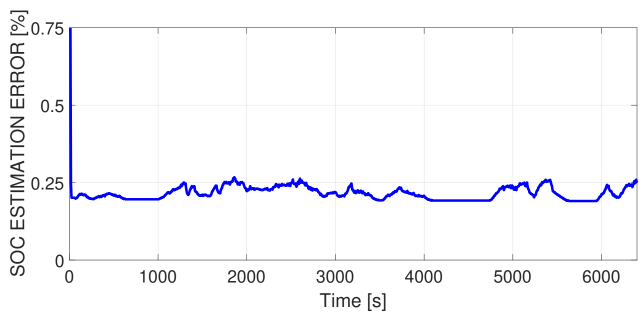

Figure 12: SOC estimation error for the WLTP

References

[1] X. Luo, J. Wang, M. Dooner, J. Clarke, Overview of current development in electrical energy storage technologies and the application potential in power system operation, Applied Energy 137 (2015) 511–536.

[2] E. V. I. (EVI), Global ev outlook 2019 scaling up the transition to electric mobility, IEA (2019).

[3] A. Schmidt, A. Smith, H. Ehrenberg, Power capability and cyclic aging of commercial, high power lithium ion battery cells with respect to different cell designs, Journal of Power Sources 425 (2019) 27–38.

Table 2: Maximum error and convergence time according to the initial conditions of the estimated SOC

SOC_{estim} at $t = 0$	$Error_{max}(\%)$	$t_{convergence}$ (s)
100%	0.252	0
80%	0.250	29.2
60%	0.263	41.3
20%	0.301	55.9

[4] F. Lv, Z. Wang, L. Shi, J. Zhu, K. Edstrom, J. Mindemark, S. Yuan, Challenges and development of composite solid-state electrolytes for high-performance lithium-ion batteries, Journal of Power Sources 441 (2019).

[5] Q. Lin, J. Wang, R. Xiong, W. S. H. He, Towards a smarter battery management system: A critical review on optimal charging methods of lithium ion batteries, Energy 183 (2019) 220–234.

[6] H. Ren, Y. Zhao, S. Chen, T. Wang, Design and implementation of a battery management system with active charge balance based on the SOC and SOH online estimation, Energy 166 (2019) 908–917.

[7] K. Lim, H. A. Bastawrous, V.-H. Duong, K. W. See, P. Zhang, S. X. Dou, Fading kalman filter-based real-time state of charge estimation in LiFePO4 battery-powered electric vehicles, Applied Energy 169 (2016) 40–48.

[8] P. Shrivastava, T. K. Soon, , M. Y. I. B. Idris, S. Mekhilef, Overview

of model-based online state-of-charge estimation using kalman filter family for lithium-ion batteries, Renewable and Sustainable Energy Reviews 113 (2019).

[9] A. Farmann, W. Waag, A. Marongiu, D. U. Sauer, Critical review of on-board capacity estimation techniques for lithium-ion batteries in electric and hybrid electric vehicles, Journal of Power Sources 281 (2015) 114–130.

[10] M. U. Cuma, T. Koroglu, A comprehensive review on estimation strategies used in hybrid and battery electric vehicles, Renewable and Sustainable Energy Reviews 42 (2015) 517–531.

[11] K. S. Ng, C.-S. Moo, Y.-P. Chen, Y.-C. Hsieh, Enhanced Coulomb counting method for estimating state-of-charge and state-of-health of lithium-ion batteries, Applied Energy 86 (2009) 1506–1511.

[12] B. Pattipati, B. Balasingam, G. Avvari, K. Pattipati, Y. Bar-Shalom, A review on lithium-ion battery ageing mechanisms and estimations for automotive applications, Journal of Power Sources 269 (2014) 317–333.

[13] M. Coleman, C. K. Lee, C. Zhu, W. G. Hurley, A review on lithium-ion battery ageing mechanisms and estimations for automotive applications, IEEE Transactions on Industrial Electronics 54 (2007) 2550–2557.

[14] A. E. Mejdoubi, A. Oukaour, H. Chaoui, H. Gualous, J. S. Y. Slamani, State-of-charge and state-of-health lithium-ion batteriesâ diagnosis according to surface temperature variation, IEEE Transactions on Industrial Electronics 63 (2016) 2391 – 2402.

[15] F. Codeca, S. M. Savaresi, V. Manzoni, The mix estimation algorithm for battery state-of-charge estimator- analysis of the sensitivity to measurement errors., in: Proceedings of the 48h IEEE Conference on Decision and Control (CDC) held jointly with 2009 28th Chinese Control Conference, 2009, pp. 8083–8088.

[16] M. A. Roscher, D. U. Sauer, Dynamic electric behavior and open-circuit-voltage modeling of lifepo4-based lithium ion secondary batteries, Journal of Power Sources 196 (2011) 331–336.

[17] U. Westerhoff, T. Kroker, K. Kurbach, M. Kurrat, Electrochemical impedance spectroscopy based estimation of the state of charge of lithium-ion batteries, Journal of Energy Storage 8 (2016) 244–256.

[18] A. H. Ranjbar, A. Banaei, A. Khoobroo, B. Fahimi, Online estimation of state of charge in li-ion batteries using impulse response concept, IEEE Transactions on Smart Grid 3 (2012) 360–367.

[19] M. Fleckenstein, O. Bohlen, M. A. Roscher, B. Baker, Current density and state of charge inhomogeneities in li-ion battery cells with lifepo4 as cathode material due to temperature gradients, Journal of Power Sources 196 (2011) 4769–4778.

[20] J. Gomez, R. Nelson, E. E. Kalu, M. H. Weatherspoon, J. P. Zheng, Equivalent circuit model parameters of a high-power li-ion battery: Thermal and state of charge effects, Journal of Power Sources 196 (2011) 4826–4831.

[21] A. Zenati, P. Desprez, H. Razik, Estimation of the soc and the soh of li-ion batteries, by combining impedance measurements with the fuzzy logic inference, in: IECON 2010 - 36th Annual Conference on IEEE Industrial Electronics Society, 2010, pp. 1773–1778.

[22] P. Singh, C. F. Jr., D. Reisner, Fuzzy logic modelling of state-of-charge and available capacity of nickel/metal hydride batteries, Journal of Power Sources 136 (2004) 322–333.

[23] S. Tong, J. H. Lacap, J. W. Park, Battery state of charge estimation using a load-classifying neural network, Journal of Energy Storage 7 (2016) 236–243.

[24] B. Xia, D. Cui, Z. Sun, Z. Lao, R. Zhang, W. Wang, W. Sun, Y. Lai, M. Wang, State of charge estimation of lithium-ion batteries using optimized levenberg-marquardt wavelet neural network, Energy 153 (2018).

[25] H. B. Sassi, F. Errahimi, N. Es-Sbai, C. Alaoui, Comparative study of ann/kf for on-board soc estimation for vehicular applications, Journal of Energy Storage 25 (2019).

[26] S. Xing, W. He, M. Pecht, K. L. Tsui, State of charge estimation of lithium-ion batteries using the open-circuit voltage at various ambient temperatures, Applied Energy 113 (2014) 106–115.

[27] X. Liu, Z. Chen, C. Zhang, J. Wu, A novel temperature-compensated model for power li-ion batteries with dual-particle-filter state of charge estimation, Applied Energy 123 (2014) 263–272.

[28] W. Waag, C. Fleischer, D. U. Sauer, Critical review of the methods for monitoring of lithium-ion batteries in electric and hybrid vehicles, Journal of Power Sources 258 (2014) 321–339.

[29] J. E. Bester, A. E. Hajjaji, A. M. Mabwe, Modelling of lithium-ion battery and soc estimation using simple and extended discrete kalman filters for aircraft energy management, in: IECON 2015 - 41st Annual Conference of the IEEE Industrial Electronics Society, 2015, pp. 2433–2438.

[30] R. Xiong, F. Sun, Z. Chen, H. He, A data-driven multi-scale extended kalman filtering based parameter and state estimation approach of lithium-ion olymer battery in electric vehicles, Applied Energy 113 (2014) 463–476.

[31] J. Li, J. K. Barillas, C. Guenther, M. A. Danzer, A comparative study of state of charge estimation algorithms for lifepo4 batteries used in electric vehicles, Journal of Power Sources 230 (2013) 244–250.

[32] G. L. Plett, Sigma-point kalman filtering for battery management systems of lipb-based hev battery packs part 1: Introduction and state estimation, Journal of Power Sources 161 (2006).

[33] A. Valade, P. Acco, P. Grabolosa, , J.-Y. Fourniols, A study about kalman filters applied to embedded sensors, Sensors 212 (2017).

[34] M. Hannan, M. Lipu, A. Hussain, A. Mohamed, A review of lithium-ion battery state of charge estimation and management system in electric vehicle applications: Challenges and recommendations, Renewable and Sustainable Energy Reviews 78 (2017).

[35] M. Ye, H. Guo, R. Xiong, Q. Yu, A double-scale and adaptive particle filter-based online parameter and state of charge estimation method for lithium-ion batteries, Energy (2017).

[36] S. Li, S. Pischinger, C. He, L. Liang, M. Stapelbroekb, A comparative study of model-based capacity estimation algorithms in dual estimation frameworks for lithium-ion batteries under an accelerated aging test, Applied Energy 212 (2018).

[37] Y. Yang, N. Cui, C. Wang, M. Liu, R. Gao, Soc estimation of lithium-ion battery based on new adaptive fading extended kalman filter, in: 2017 Chinese Automation Congress (CAC), 2017.

[38] Y. Huangfu, J. Xu, S. Zhuo, M. Xie, Y. Liu, A novel adaptive sliding mode observer for soc estimation of lithium batteries in electric vehicles, in: 2017 7th International Conference on Power Electronics Systems and Applications - Smart Mobility, Power Transfer Security (PESA), 2017.

[39] K. V. Singh, H. O. Bansal, D. Singh, Hardware-in-the-loop implementation of anfis based adaptive soc estimation of lithium-ion battery for hybrid vehicle applications, Journal of Energy Storage 27 (2020).

[40] R. A. El-Sehiemy, M. Hamida, T. Mesbahi, Parameter identification and state-of-charge estimation for lithium-polymer battery cells using enhanced sunflower optimization algorithm, Journal of Energy Storage 45 (2020) 8833–8842.

[41] D. Ouyang, J. Weng, M. Chen, J. Wang, Impact of high-temperature environment on the optimal cycle rate of lithium-ion battery, Journal of Energy Storage 28 (2020).

[42] H. He, R. Xiong, H. Guo, S. Li, Comparison study on the battery models used for the energy management of batteries in electric vehicles, Energy Conversion and Management 64 (2012) 113–121.

[43] C. Ozkurt, F. Camci, V. Atamuradov, C. Odorry, Integration of sampling based battery state of health estimation method in electric vehicles, Applied Energy 175 (2016) 356–367.

[44] J. Snoussi, S. B. Elghali, R. Outbib, M. F. Mimouni, Sliding mode control for frequency-based energy management strategy of hybrid storage system in vehicular application, in: 2016 International Symposium on Power Electronics, Electrical Drives, Automation and Motion (SPEEDAM), 2016, pp. 1109–1114.

[45] T. Bruen, J. Marco, Modelling and experimental evaluation of parallel connected lithium ion cells for an electric vehicle battery system, Journal of Power Sources 310 (2016) 91–101.

[46] S. Zhang, R. Xiong, J. Cao, Battery durability and longevity based power management for plug-in hybrid electric vehicle with hybrid energy storage system, Applied Energy 179 (2016) 316–328.

[47] T. Mesbahi, F. Khenfri, N. Rizoug, K. Chaaban, P. Bartholomeus, P. L. Moigne, Dynamical modeling of li-ion batteries for electric vehicle applications based on hybrid particle Swarm Nelder Mead (PSONM) optimization algorithm, Electric Power Systems Research 131 (2016) 195–204.

[48] X. Hu, S. Li, H. Peng, A comparative study of equivalent circuit models for li-ion batteries, Journal of Power Sources 198 (2012).

[49] C. Y. Chun, J. Baek, G.-S. Seo, B. Cho, J. Kim, I. K. Chang, S. Lee, Current sensor-less state-of-charge estimation algorithm for lithium-ion batter-

ies utilizing filtered terminal voltage, Journal of Power Sources 273 (2015) 255–263.

[50] H. Rahimi-Eichi, F. Baronti, M.-Y. Chow, Online adaptive parameter identification and state-of-charge coestimation for lithium-polymer battery cells, IEEE Transactions on Industrial Electronics 61 (2014) 2053–2061.

[51] M. Mandal, A. Asif, Continuous and Discrete Time Signals and Systems, CAMBRIDGE UNIVERSITY PRESS, United States of America, New York, 2007.

[52] M. Darouach, M. Zasadzinski, S. J. Xu, Full-order observers for linear systems with unknown inputs, IEEE Transactions on Automatic Control 39 (1994) 606–609.

[53] M. Zerrougui, M. Darouach, L. Boutat-Baddas, H. Souley-Ali, H_∞ filtering for singular bilinear systems with application to a single-link flexible-joint robot, International Journal of Control, Automation and Systemss 12 (2014) 590–598.

[54] M. Darouach, L. Boutat-Baddas, M. Zerrougui, H_∞observers design for a class of nonlinear singular system, Automatica 47 (2011) 2517–2525.

[55] M. C. Nguyen, H. Trinh, Unknown input observer design for one-sided lipschitz discrete-time systems subject to time-delay, Applied Mathematics and Computation 286 (2016) 57 – 71.

[56] B. Zhou, G.-R. Duan, A new solution to the generalized sylvester matrix equation $av - evf = bw$, Systems Control Letters 55 (2006) 193 – 198.

[57] W. Zhang, L. Wang, L. Wang, C. Liao, An improved adaptive estimator for state-of-charge estimation of lithium-ion batteries, Journal of Power Sources 402 (2018).

[58] D. Li, J. Ouyang, H. Li, J. Wan, State of charge estimation for $LiMn_2O_4$ power battery based on strong tracking sigma point kalman filter, Journal of Power Sources 279 (2015).